POLYMERS FOR ADVANCED TECHNOLOGIES
Polym. Adv. Technol. 2006; **17**: 272–280
Published online 16 January 2006 in Wiley InterScience (www.interscience.wiley.com). DOI: 10.1002/pat.697

PAT

The thermal degradation of poly(methyl methacrylate) nanocomposites with montmorillonite, layered double hydroxides and carbon nanotubes†

Marius C. Costache[1], Dongyan Wang[2], Matthew J. Heidecker[3], E. Manias[3] and Charles A. Wilkie[1]*

[1]Department of Chemistry, Marquette University, PO Box 1881, Milwaukee, WI 53201, USA
[2]Department of Materials Science & Engineering, Cornell University, Ithaca, NY 14853, USA
[3]Department of Materials Science & Engineering, Penn State University, 325-D Steidle Bldg, University Park, PA 16802, USA

Received 5 May 2005; Revised 18 October 2005; Accepted 3 November 2005

The thermal degradation of poly(methyl methacrylate) and its nanocomposite has been studied to determine if the presence of clays (anionic and cationic) or carbon nanotubes has an effect on the degradation pathway. Nanocomposite formation has been established by X-ray diffraction and transmission electron microscopy, thermal degradation has been investigated by cone calorimetry and thermogravimetric analysis (TGA), and the products of degradation have been studied with TGA/FT-IR and gas chromatography/mass spectrometry (GC/MS). There are no marked differences in the degradation products of the polymer and its nanocomposites, but the degradation of the nanocomposite occurs at higher temperatures. The most likely explanation is that poly(methyl methacrylate) degrades by only a single route, so the clay cannot promote one pathway at the expense of another. This observation bears important implications for the barrier mechanism, which is currently used to explain the reduction in the peak heat release rate of nanocomposites.

KEYWORDS: poly(methyl methacrylate); nanocomposites; cone calorimetry; thermal properties; clay

INTRODUCTION

Polymer layered silicate nanocomposites have drawn the attention of researchers because of their unique behavior; the addition of only a very limited amount of clay (usually less than 5% inorganic) to a polymeric matrix has a significant impact on the mechanical, thermal, fire and barrier properties of the polymer.[1–3] Of particular interest is polymer nanocomposite flammability, the reduction in the peak heat release rate (PHRR) is dependent on the polymer matrix. In the case of polystyrene (PS), polyamide-6 (PA-6) and ethylene-vinyl acetate copolymer (EVA), the reduction in PHRR is quite significant, usually about 60%. However, in the case of poly(methyl methacrylate), only a modest reduction in PHRR, perhaps 25%, can be achieved.

To explain the observed reduction in polymer flammability, two mechanisms have been suggested: barrier formation[4] (the widely accepted theory for the reduction of PHRR) and paramagnetic radical trapping.[5] X-ray photoelectron spectroscopy (XPS) studies of polymer-clay nanocomposites[6–8] have shown that during thermal degradation the apparent concentration of clays at the surface increases as the organic material decomposes. This high clay concentration char, which builds up on the surface during burning, acts as a barrier—slowing the mass loss rate of the decomposition products and also insulating the underlying material from heat. Recent work from this laboratory[9–13] has shown that the barrier improvements could also have another effect on the polymer's thermal decomposition. The delay in the evolution of the degraded species can lead to extensive scission accompanied by recombination, or other intermolecular reactions, resulting in multiple bond formation and/or crosslinking, all associated with increased thermal stability and, therefore, a reduced PHRR. The paramagnetic radical trapping mechanism seems to be important only when the clay cannot provide an effective barrier improvement, as in nanocomposites where the filler loading is quite low or the filler clusters are very large. However, if these were the only two processes by which the heat release rate is influenced, one might expect that the reduction would be similar across different nanocomposite systems, regardless of the identity of the polymer.

While the polymer layered silicate nanocomposites are more thoroughly studied, polymer layered double hydroxides are emerging as a new class of materials suitable for a wide range of applications.[14] Layered double hydroxides (LDHs), also known as hydrotalcite-like materials, belong to the large class of anionic clays and are characterized by a high

**Correspondence to*: C. A. Wilkie, Department of Chemistry, Marquette University, PO Box 1881, Milwaukee, WI 53201, USA.
E-mail: Charles.wilkie@marquette.edu
†Paper presented as part of a special issue on nanocomposites and flame retardancy.

surface area. Even though they are less abundant in nature than their cationic counterparts, their synthetic preparation is facile through a variety of methods,[15–17] making them readily available. The structure of these hydrotalcite-like materials can be easily understood starting from the structure of brucite,[18] $Mg(OH)_2$, where octahedra of Mg^{2+} (six-fold coordinated to HO^-) share edges to form infinite sheets that are stacked together by hydrogen bonding. When a trivalent cation, such as Al^{3+}, substitutes for a Mg^{2+}, a positive charge is generated in the hydroxyl sheet. This positive charge is balanced by the insertion of exchangeable anions between the brucite-like sheets, most commonly carbonate. Other anions, which can render the material more organophilic, are also possible through ion exchange.

Extensive degradation studies on poly(methyl methacrylate)(PMMA) have been carried out,[19–22] and two mechanisms are generally accepted for the initiation of the degradation: main chain random scission[19–21] and the homolytic scission of the methoxycarbonyl side group.[22] In the first case, an isobutyryl macroradical is formed (followed by an effective β scission with monomer generation), along with a primary macroradical which is believed to undergo a β elimination with the formation of methallyl-terminated PMMA, CO, CO_2, methoxy and methyl radicals. In the second mechanism, upon homolytic scission of the methoxycarbonyl group, the remaining polymer radical can undergo β scission to afford an isobutyryl macroradical (that will effectively depolymerize) and a methallyl-terminated PMMA chain. The newly formed radical can then cleave to give another isobutyryl macroradical, which will depolymerize, and a series of small molecules, which depend upon the small radicals formed in the previous step. A series of recombination/disproportionation products are identified in the degradation products. Regardless of the mechanism of the initiation step, the degradation product is almost exclusively a methyl methacrylate (MMA) monomer (>99%).[23]

There have been a few previous studies on the cone calorimetry on PMMA-clay nanocomposites.[24,25] The typical reduction in the PHRR is in the range of 20 to 30% and it seems to be dependent on both the identity and amount of the surfactant. Surprisingly, the time-to-ignition does not seem to show the same decrease that is seen for most other polymers and, in fact, may increase in a few cases.

The objective of this study is to examine the effect of different inorganic fillers [cationic and anionic clays and multi-wall carbon nanotubes (CNTs)] and the respective nanocomposite morphologies on the degradation pathway of PMMA, and to identify the products of the thermal degradation.

EXPERIMENTAL

Materials

Benzoyl peroxide (97%), sodium 4-styrenesulfonate, 2-aminotoluene-5-sulfonic acid (97%) and monomeric MMA (99%) were obtained from the Aldrich Chemical Co., Inc. Monomer was used after it was passed through a column packed with inhibitor-remover for *t*-butylcatechol, also purchased from Aldrich. Tetrahydrofuran (THF, 99+%), was purchased from Alfa Aesar and Cloisite 30B (montmorillonite cation exchanged with methyl tallow bis(2-hydroxyethyl) ammonium) was kindly provided by Southern Clay Products Inc. Multi-wall CNTs were kindly provided by Olivier Decroly, Nanocyl S.A., Belgium. All of these were used without prior purification. The organically modified LDHs used were derived from Pural MG63HT (magnesium-aluminum LDS intercalated with carbonate anion), kindly provided by Sasol.

Anion exchange of layered double hydroxides (LDHs)

In a round bottom flask 1000 ml of distilled water was degassed by bubbling nitrogen through for 20 min. After 20 g LDH-carbonate was added and stirred vigorously for 2 hr, then 20 g of sodium 4-styrenesulfonate (StSA) was added and the evolution of CO_2 was observed. The pH of 5 was maintained by addition of small amounts of dilute HCl and the suspension was stirred overnight, then filtered under nitrogen, washed with distilled, degassed water and dried in a vacuum oven at 50°C to afford the organically modified LDH (MStSA). A similar procedure was used for 2-aminotoluene-5-sulfonic acid (ATSA), affording the corresponding modified LDH (MATSA). The modification was confirmed by X-ray diffraction (XRD) and FT-IR on KBr pellet (see Figs. 1 and 2, respectively). The basal *d*-spacing of the LDH (d_{003}) increased upon modification from 0.76 to 1.67 nm for MATSA and 1.88 nm for MStSA (Fig. 1). Also, FT-IR shows in both cases the almost complete disappearance of the carbonate (1369 cm^{-1}) and the presence of the characteristic sufonate peaks in the 1240–960 cm^{-1} region.

Preparation of nanocomposites

The inorganic loading was kept constant at 3% for all the clay-nanocomposite systems. A bulk polymerization technique was utilized for the preparation of the PMMA nanocomposite; the filler (4% Cloisite 30B, 3% CNT or 7% organically modified LDHs) was dispersed for 24 hr in MMA; after the addition of the benzoyl peroxide initiator, the mixture was

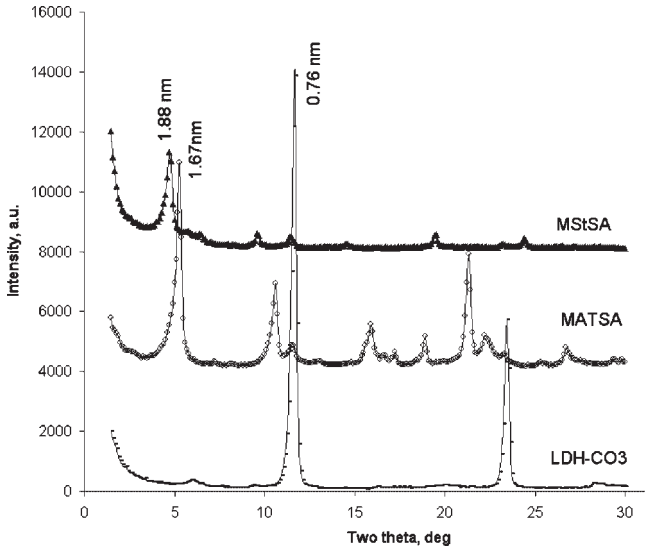

Figure 1. XRD patterns of organically modified and carbonate LDHs.

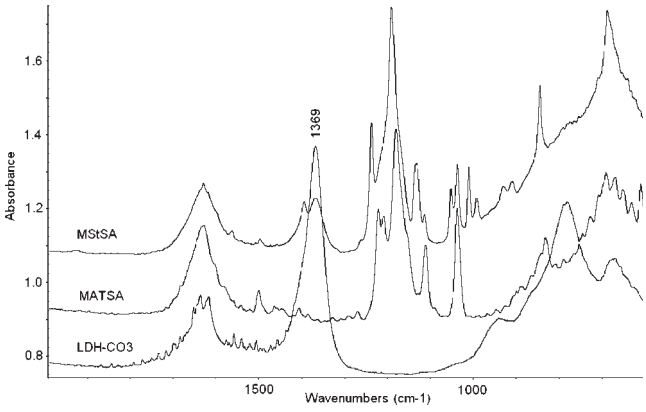

Figure 2. Selected FT-IR (KBr pellet) of organically modified and carbonate LDHs.

heated to 70°C for 24 hr. The nanocomposite was recovered then the product was placed in a vacuum oven at 80°C overnight. A detailed procedure can be found in the literature.[26] The virgin polymer was prepared by an identical procedure, in the absence of the inorganic fillers.

Characterization of nanocomposites

XRD, transmission electron microscopy (TEM), cone calorimetry and thermogravimetric analysis (TGA) were used to characterize the nanocomposites. XRD patterns were obtained using a Rigaku Geiger Flex, 2-circle powder diffractometer equipped with Cu-K_α generator (λ=1.5404 Å); generator tension was 50 kV and the current was 20 mA. TEM images of the PMMA-Cloisite 30B sample were obtained at 60 kV with a Zeiss 10c electron microscope; the samples were microtomed using a Richert-Jung Ultra-Cut E microtome. Bright field TEM images of the CNT and the LDH samples were obtained with a JEOL 1200 EXII operated with an accelerating voltage of 80 kV, and equipped with a Tietz F224 digital camera. Ultrathin sections (70–100 nm) of the nanocomposites were obtained with an ultramicrotome (Leica Ultracut UCT) equipped with a diamond knife. The sections were transferred to carbon-coated copper grids (200-mesh). Cone calorimetry measurements were performed on an Atlas CONE2 instrument, according to ASTM E 1354 at an incident flux of 50 kW/m^2 using a cone shaped heater. The spark was continuous until the sample ignited and the exhaust flow rate was 24 l/sec. The specimens for cone calorimetry were prepared by the compression molding of the sample (about 30 g) into 3mm×100mm×100 mm plaques. Typical results from cone calorimetry are reproducible to within ±10%. TGA was carried out in nitrogen, at a heating rate of 20°C/min and a nitrogen flow of 60 ml/min on a Cahn TG 131 instrument.

TGA/FT-IR analysis and sampling of evolved products

TGA/FT-IR studies were performed under nitrogen flow (60 ml/min) on a Cahn TG 131 instrument that was connected to a Mattson Research grade FT-IR through heated stainless steel tubing. The heating rate was 20°C/min and final temperature was 650°C. Volatile degradation products were sampled using a ''sniffer'' tube that extends into the sample cup to remove the evolved gases at a rate of 40 ml/min. The evolved volatile products were introduced to the IR chamber through the heated stainless steel tubing and analyzed by *in situ* vapor phase FT-IR. The sample size was 40–60 mg. The temperature reproducibility of TGA is ±3°C and the fraction of non-volatile is ±3%. The evolved products during thermal degradation of each sample were also collected using a cold trap (dry ice-acetone) for further analysis.

Analysis of solid residue sample

Using the same apparatus described earlier, the degradation was quenched rapidly after 60% mass loss and the remaining solid residues were collected. The samples were then sonicated for 2 hr in the solvent of choice for each experiment (acetonitrile, chloroform or $CDCl_3$) and centrifuged for another 3 hr. These samples were subsequently analyzed by solution FT-IR using a Nicolet Magna Model 560 spectrometer, UV spectroscopy using a Shimadzu UV 2501 instrument or NMR using a 300 MHz Varian instrument.

Analysis of evolved condensable products

The evolved products collected as described earlier in the cold trap were washed with acetonitrile. Gas chromatrography/mass spectrometry (GC/MS) data were obtained using an Agilent 6850 series GC connected to an Agilent 5973 Series MS (70 eV electron ionization) with temperature programming from 40 to 250°C.

RESULTS AND DISCUSSION

Nanocomposite characterization

The clay dispersion was evaluated by XRD, TEM and cone calorimetry. In the XRD trace of the PMMA/Cloisite 30B hybrid, the basal spacing increased from 1.8 nm in Cloisite 30B clay to 3.3 nm in the nanocomposite. The d_{002} and d_{003} peaks, indicative of highly-ordered intercalated nanocomposite formation, can also be observed, as shown in Fig. 3. Likewise, the increase in the basal spacing of MStSA from 1.88 to 2.10 nm in PMMA/MStSA suggests some degree of intercalation. In contrast, the *d*-spacing does not change at all for MATSA, which may suggest that an immiscible nanocomposite has been produced. Since both ATSA and StSA are relatively small molecules compared to the typical organic modifiers used in cationic clays, it is possible that the organophilicity is insufficient to permit entry of the polymer into the

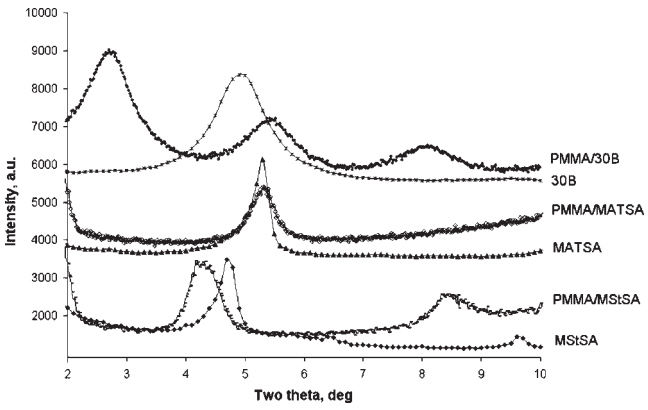

Figure 3. XRD trace of PMMA/clay nanocomposites.

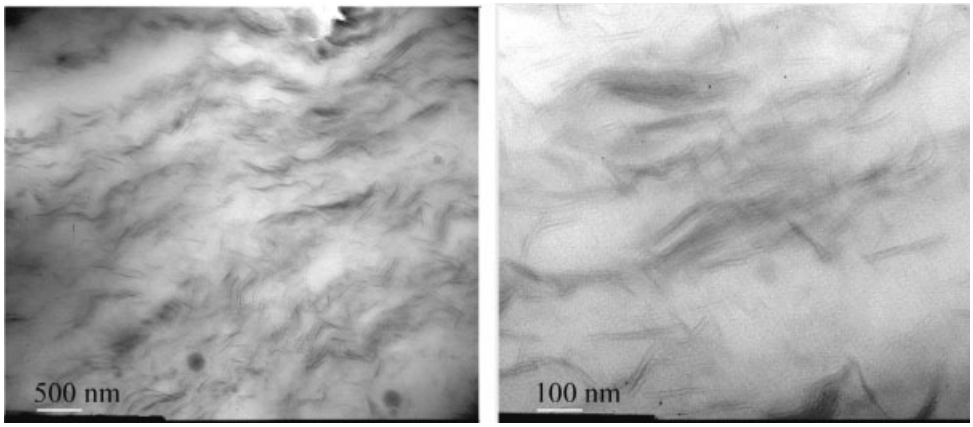

Figure 4. TEM images of PMMA/Cloisite 30B nanocomposite at low (left) and high magnification (right).

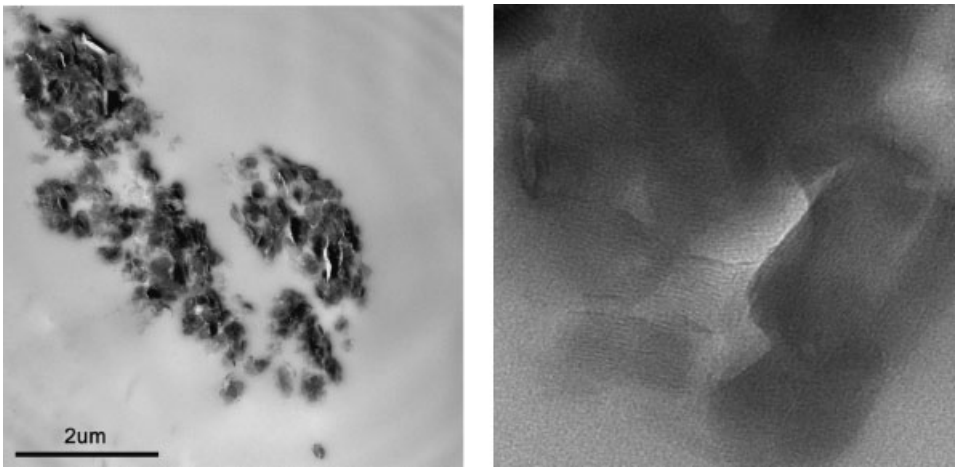

Figure 5. TEM images of PMMA/MStSA at various magnifications: the left shows a low magnification image while the right is a higher resolution (230 nm×230 nm) image of a selected region from a higher magnification image illustrating the intercalated structure.

gallery space, leading to relatively modest intercalation of the polymer.

Using (XRD) alone to characterize nanocomposite formation can often be misleading, since XRD cannot detect layers that are not in parallel registry or one-dimensional objects like the CNTs. At a minimum, XRD should be accompanied by TEM, which can provide direct imaging of the nanocomposite structure and filler dispersion, therefore affording the capability to assess—at least locally within the TEM images—the extend of nano-dispersion and ascertain whether or not the clay layers are in registry (intercalation versus delamination). The TEM images of all these PMMA nanocomposites are shown in Figs. 4–7. In the case of PMMA/Cloisite 30B very good nano-dispersion is apparent and some small tactoids are present in this intercalated material (Fig. 4).

In general, (TEM) imaging of the two PMMA/modified-LDHs (Figs. 5 and 6) shows the typical behavior for polymer/LDH nanocomposite materials, and a worse dispersion than the montmorillonite nanocomposites (Fig. 4). Namely, the LDH layers are stacked together in tactoids (composed of tens of single layers in parallel registry, reminiscent of the organically-modified LDH fillers). These tactoids in turn are grouped together in micron-sized agglomerates (Figs. 5 and 6). Of particular importance is the complete absence of any exfoliated LDH layers in either of the two systems.

More specifically, for the PMMA/MStSA TEM shows the typical morphology observed in intercalated PMMA/LDH

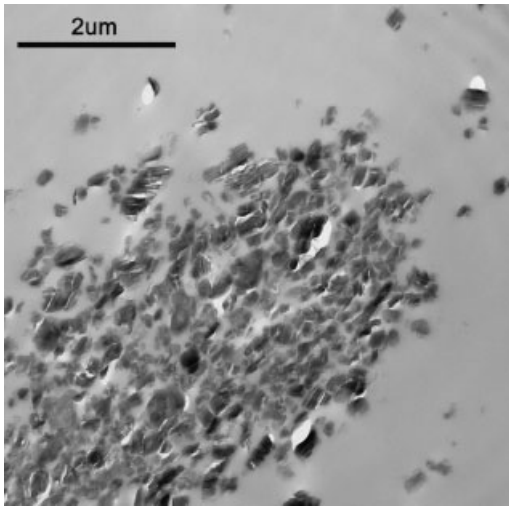

Figure 6. TEM image of PMMA/MATSA at low magnification.

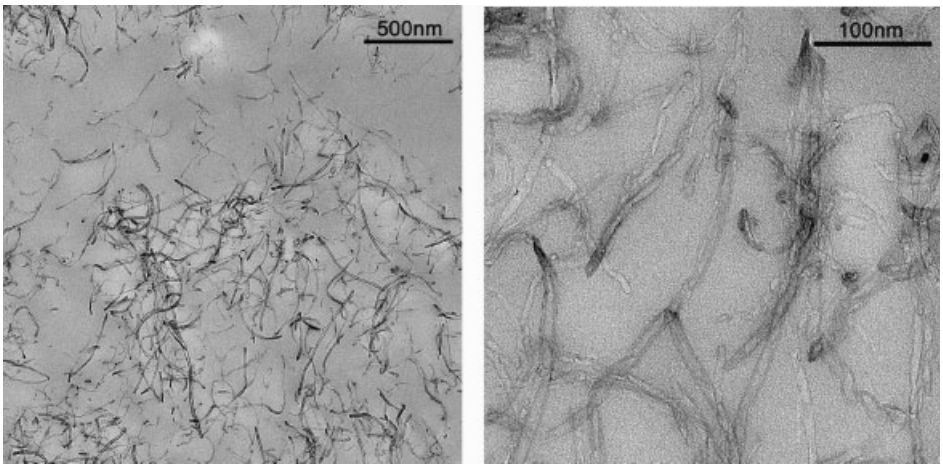

Figure 7. TEM images of PMMA/CNT at various magnifications.

composites[27] (Fig. 5), showing LDH tactoids clustered together in bigger agglomerates. Higher magnification TEM images clearly show the intercalated structure, corroborating the XRD result (Fig. 3); cone calorimetry data (*vide infra*) leads to the conclusion that an intercalated nanocomposite was obtained. For the PMMA/MATSA (Fig. 6), TEM reveals a similar microcomposite structure as for PMMA/MStSA, with the LDH layers agglomerated in stacks of 1 to 6 microns in size, which are composed of a collection of much smaller tactoids (0.1 to 0.5 micron, Fig. 6, higher magnification images). Although it was not possible to distinguish by TEM whether the layers within each tactoids are intercalated by PMMA, the XRD data strongly suggests that there is no polymer intercalation for this composite. In concert with the XRD results, TEM suggests a slightly better dispersion for PMMA/MStSA than for PMMA/MATSA at the nanometer scale (i.e. within and between the tactoids), but the micrometer scale structure is qualitatively the same.

For PMMA/CNT excellent dispersion is observed at all length scales (Fig. 7). Nanotube bundles are not observed anywhere in the composite material, and the nanotubes themselves are highly dispersed in a haphazard manner, homogeneously throughout the organic matrix, bearing no memory of their prior bundled state. There have been reports which suggest that some of the double bonds of the CNTs could break homolytically upon heating in the presence of an initiator,[28] followed by chain propagation reactions, which may in turn improve the nanotube dispersion in the *in situ* polymerized PMMA matrix.

Cone calorimetry is widely used to evaluate fire performance and it has been noted that a microcomposite gives a minimal reduction in the PHRR while nanocomposite formation brings about a larger reduction.[29–31] The heat release rate curves for PMMA and its nanocomposites are shown in Fig. 8 and all of the cone calorimetric data is presented in Table 1. The reduction in PHRR for PMMA nanocomposites is in the range 27–35% (typical for this polymer[32]) regardless of the filler used (cationic and anionic clay or CNT). PMMA/MATSA, the microcomposite, exhibits a smaller PHRR reduction, but still fairly comparable to that of the other systems. This interesting observation should be compared to the results found by Camino *et al.*,[33] who compared the fire properties of EVA-LDH with EVA-alumina trihydrate (ATH) and EVA-magnesium hydroxide (MDH). They explained that the LDH used could be viewed as a nanoscale mixture of ATH and MDH, two very well known fire retardants. Their efficiency at such a low loading, compared with the amounts usually employed, could be due to their better dispersion as compared to ATH and MDH. So in the case of the LDH samples, one may attribute the reduction in the PHRR either to nanocomposite formation or the presence of magnesium and aluminum hydroxides. The total heat released is relatively constant for all systems, which is also typical of nanocomposites. It is also worth noting the increased time-to-ignition in the case of PMMA/CNT; Kashiwagi *et al.* have previously studied PMMA-single walled nanotubes at 50 kW/m^2 and have not found this increase in the time-to-ignition.[34] It is not known if the difference is due to the difference between single-walled and multi-walled nanotubes or if there is some other explanation.

TGA curves of PMMA and its nanocomposites are presented in Fig. 9. The onset temperature (temperature at 10% mass loss, $T_{0.1}$) is increased for all nanocomposites, by 19°C for PMMA/MATSA and PMMA/MStSA, 35°C for PMMA/Cloisite 30B and 62°C for PMMA/CNT, compared

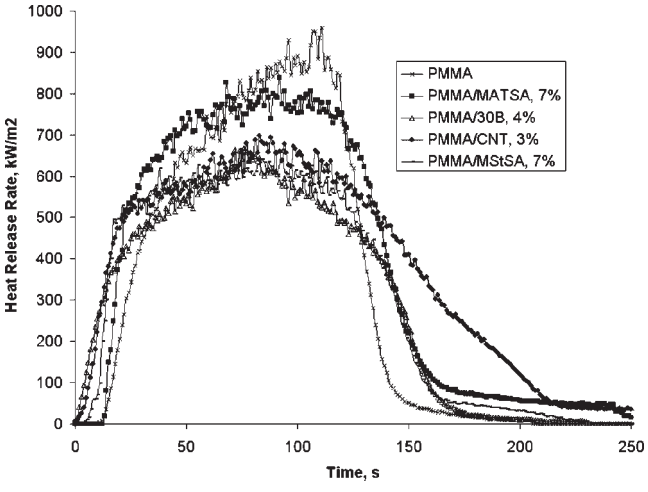

Figure 8. Heat release rate curves for PMMA and its nanocomposites at an incident heat flux of 50 kW/m^2.

Table 1. Cone calorimetry data, at an incident heat flux of 50 kW/m^2, for PMMA and its nanocomposites

Composition	PHRR (kW/m^2) (reduction, %)	THR (MJ/m^2)	ASEA (m^2/kg)	AMLR (g/sec m^2)	t_{ign} (sec)
PMMA	982 ± 20	83 ± 3	150 ± 5	31.5 ± 0.3	16 ± 2
PMMA/MATSA	809 ± 15 (18%)	91 ± 6	176 ± 3	21.4 ± 0.1	12 ± 2
PMMA/Cloisite 30B	638 ± 14 (35%)	74 ± 1	177 ± 1	21.7 ± 0.1	4 ± 1
PMMA/CNT	682 ± 18 (29%)	96 ± 3	138 ± 20	17.5 ± 1.3	40 ± 4
PMMA/MStSA	654 ± 11 (33%)	81 ± 2	164 ± 22	17.9 ± 0.8	11 ± 1

Note: PHRR. peak heat release rate; THR, total heat released; ASEA, average specific extinction area (a measure of smoke produced); AMLR, average mass loss rate; t_{ign}, time-to-ignition.

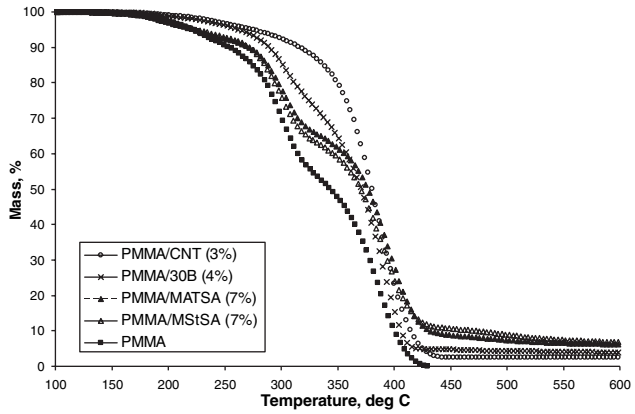

Figure 9. TGA curves of PMMA and its nanocomposites.

to virgin PMMA. The mid-point temperature (temperature at 50% mass loss, $T_{0.5}$) is increased compared to virgin PMMA by namely 30°C for all the composites studied, in agreement with previous observations on PMMA nanocomposites,[32] and the various nano-fillers had no marked effect on the $T_{0.5}$ value.

There is another very interesting observation that must be noted. In the case of the clay systems, both montmorillonite and LDH, two or three steps in the degradation may be observed but for the CNTs, the degradation of PMMA proceeds by a single step. Kashiwagi *et al.* identified three steps in the thermal degradation of radically-prepared

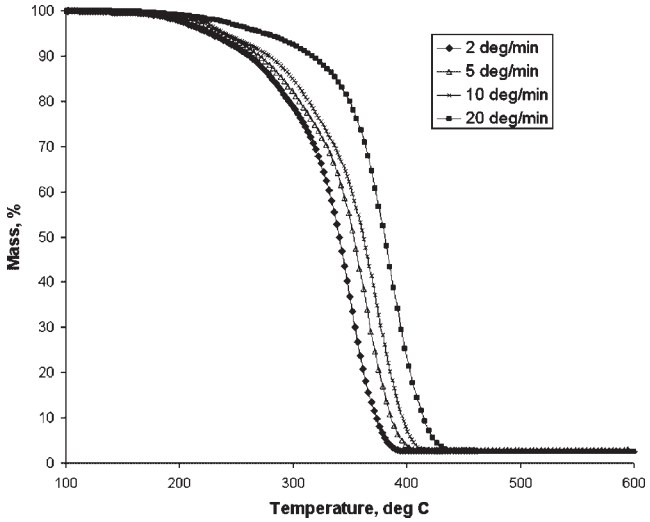

Figure 10. TGA of PMMA/CNT at various ramp rates.

PMMA, which were assigned to the presence of head-to-head linkages, end-chain unsaturation and the major step was assigned to random scission.[19] These were only seen in that study at slow ramp rates but they are obvious here even at 20°C/min. As can be seen in Fig. 10, there may be an additional step for PMMA/CNT at slower ramp rates but this effect is not as pronounced as with the PMMA/clay systems. This may suggest that the presence of CNTs has some templating effect during the synthesis of PMMA and this may reduce the formation of weak links in the structure.

Analysis of condensable evolved gases by TGA/FT-IR and GC/MS

Using the procedure described earlier, *in situ* FT-IR was performed on virgin PMMA and its nanocomposites. The spectra collected at early stages of degradation (Fig. 11) are identical to that of monomeric MMA, as expected. Moreover, no significant changes in the spectra appear over the course of degradation (spectra not shown here), suggesting that no new functionalities are evolved.

This conclusion is also supported by GC/MS data, shown in Fig. 12, which show that essentially the only degradation product from PMMA and its nanocomposites is monomeric MMA. It is of interest to note that while the onset and mid-point temperatures of the degradation, as studied by TGA in nitrogen, have been changed, the product of the degradation is only monomeric MMA. This must mean that the presence of the clay influences the temperature at which the product is evolved, but it does not change the identity of the product. For some nanocomposites, the onset temperature of degradation is increased, PS is an example[10], while for others there is no change in temperature, PA-6 for instance,[9] and for EVA[11] the temperature at which the initial degradation step occurs, which is the loss of acetic acid, is actually lower for the nanocomposite than for the virgin polymer. No satisfactory explanation has yet been put forward to explain the variation in TGA performance.

In the case of PS, EVA copolymer and PA-6 nanocomposites, either new decomposition products are formed or they are formed in quite different amounts.[9–11] These changes are attributed to modifications in the degradation pathway of those polymers, and it is clearly an effect not observed here in the degradation of the methacrylate nanocomposites.

Analysis of solid residues at 60% mass loss

The same observation that has been made for the volatiles can also be seen when the condensed phase is examined. The solution FT-IR spectra of the residue after 60% of the mass

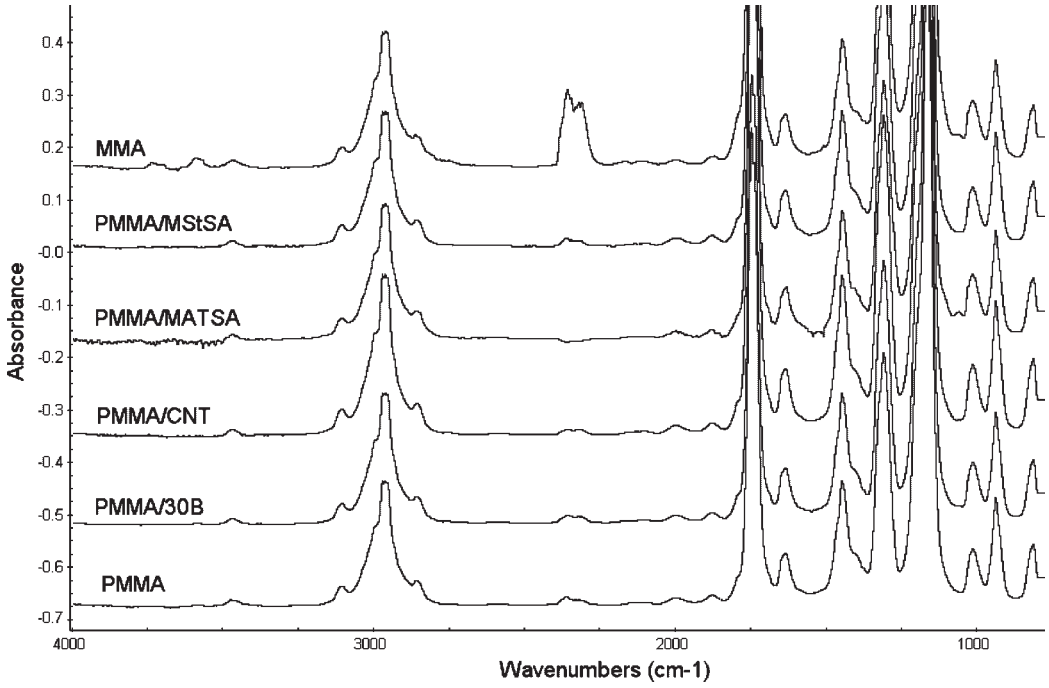

Figure 11. *In situ* vapor FT-IR spectra of evolved products from PMMA and its nanocomposites, at 30% mass loss, along with vapor phase FT-IR spectrum of MMA.

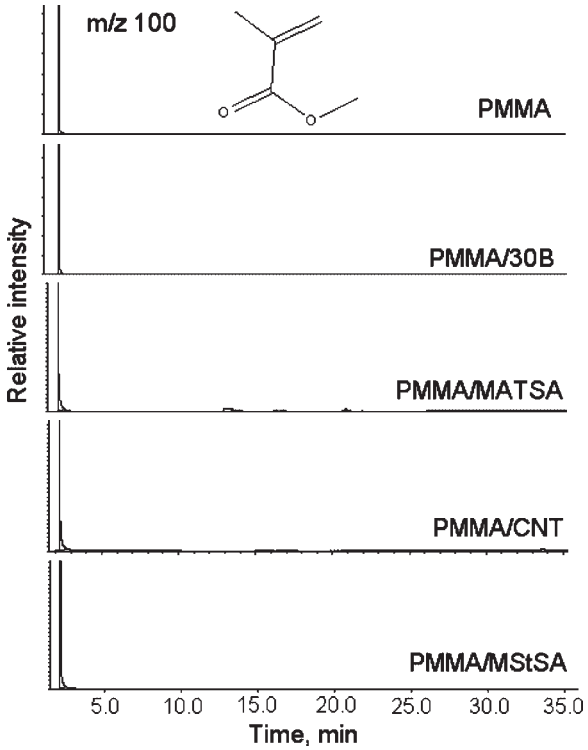

Figure 12. GC traces of condensable products trapped from degradation of PMMA and its nanocomposites.

has been lost are the same for virgin PMMA and its nanocomposite; these spectra are not shown. Likewise, the ^{1}H-NMR spectra of the residue at 60% mass loss of virgin PMMA and its nanocomposites are similar (Fig. 13). To investigate the possibility of conjugated double bond formation, the UV/Vis spectra of PMMA and its nanocomposite at 60% mass loss were compared to that of virgin PMMA and no absorption band can be observed above 240 nm for any of these samples; it can be concluded that conjugated double bonds are not formed during the degradation of PMMA or its nanocomposites. These results clearly suggest the presence of a PMMA-like structure even at relatively late stages in the degradation.

There is a significant difference between PMMA and other polymers reported previously from this laboratory, such as PA-6,[9] PS[10] and EVA.[11] In the case of the latter three polymers, there is a very large reduction in the PHRR upon nanocomposite formation, accompanied also by the observation of different decomposition products—or different quantities of products—than for the virgin polymer. In this work, the reduction in the PHRR is much smaller and the products of degradation for all nanocomposites are identical with those of the virgin polymer.

This marked deviation of the PMMA nanocomposite decomposition behavior from other polymer nanocomposites bears important implications for the general applicability of the barrier effect as the mechanism for improving flame retardancy in polymer/inorganic nanocomposites. The results and discussion outlined in this article put forward the idea that the clay qualitatively affects the polymer degradation for a number of polymers.[9–13] One can either view this effect in terms of the multiplicity of degradation pathways or in terms of radical stability. When there is more than one degradation pathway, as for instance in the case of PS where both monomer and oligomer are produced, the presence of the clay can promote one degradation pathway at the expense of another. If the pathway which is promoted leads to higher molecular weight material, then the polymer is degraded more slowly than it would be in the absence of the clay and the heat release rate curve is flattened. However, if there is

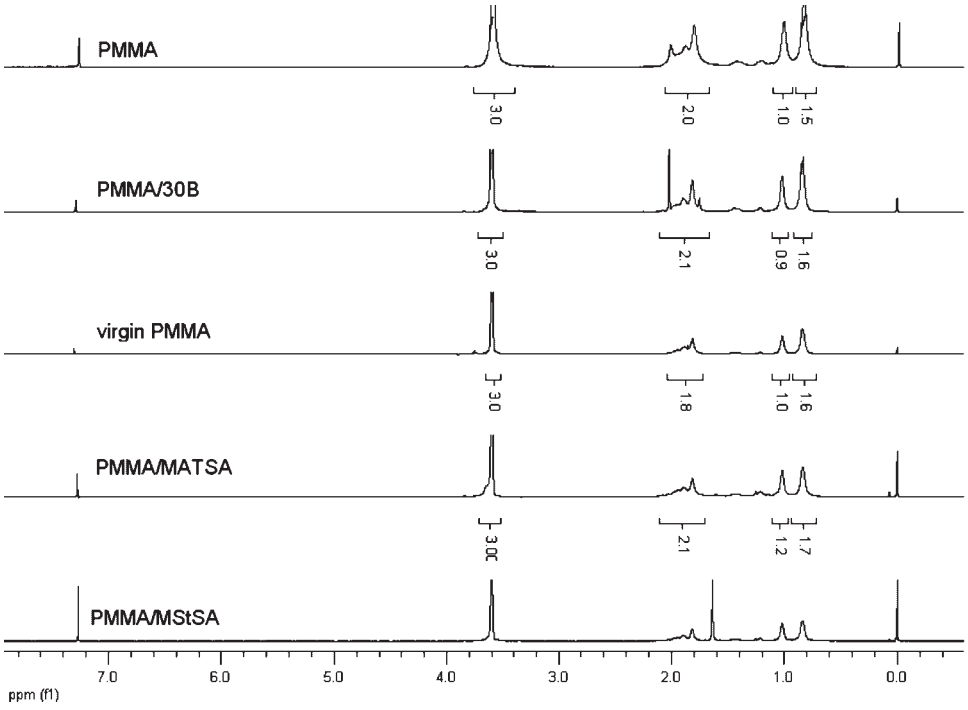

Figure 13. [1]H-NMR of the solid residue at 60% mass loss for PMMA and its nanocomposites.

only a single degradation pathway, as is the case for PMMA, the clay cannot promote a different degradation pathway and a smaller reduction in the PHRR is expected. Viewed in terms of radical stability, if a more stable radical is produced in the presence of the filler, it will have a longer lifetime, which allows for a variety of radical recombination reactions and thus reformation of polymers, and this would again result in a flattening of the heat release rate curve.[13]

In either case, altered degradation pathways or varied radical stability, these filler effects have important consequences for the design of nanocomposites with enhanced flame performance. First of all, the clay—or any other nanofiller—no longer has to rise to the surface to impact the thermal degradation of the polymer. Wherever it may exist in the matrix, it can act as a barrier to retain, for a brief time, the degrading polymer and permit more radical recombination reactions to occur. In the case of a relatively stable radical, the role of the clay is to prevent mass transport from the bulk and to permit radical recombination reactions and thus the reformation of polymers. When the radicals produced are relatively unstable, only the mass transport is prevented, since the radicals are not stable enough to participate in radical recombination reactions, and the reduction in the PHRR will not be large.

The second important consequence relates to the fact that the polymer is still combustible and, in fact, ignites earlier than the virgin polymer, despite the reduction in PHRR. Thus, it is most unlikely that nanocomposite formation alone will bring about fire retardancy in any given polymer, rather superior fire performance would necessitate the synergistic combination of nanocomposite formation with other additives or mechanisms. This becomes especially important for polymers like PMMA where nanocomposite formation yields only a modest reduction in PHRR and this suggests that nanocomposite formation may not be particularly useful as a component of a fire retardant system for PMMA.

CONCLUSIONS

The data indicates that the presence of clay (cationic or anionic) or CNTs has no qualitative effect on the degradation mechanisms of PMMA. Since PMMA undergoes thermal degradation by a single process, the presence of filler cannot change its degradation pathway, in contrast to other systems—such as PA-6, PS and EVA—where fillers can promote one thermal decomposition pathway at the expense of another. The barrier mechanism, which is the most widely-proposed mechanism by which nanocomposite formation imparts fire retardancy to polymers, is actually important not only at the surface, but also within the polymer matrix. Thus, in many cases, the reduction of mass transport is much more important than the insulating effect which arises only at the surface.

Acknowledgements

The nano-dimensional materials, Cloisite 30B, LDH and CNTs were kindly provided by Southern Clay Products, Sasol and Olivier Decroly of Nanocyl, respectively. Work at Marquette University was supported by the Habermann fund, MJH was supported through an ES&F fellowship (through Penn State's ARL).

REFERENCES

1. (a) Alexandre M, Dubois P. Polymer-layered silicate nanocomposites: Preparation, properties and uses of a new class of materials. *Mater. Sci. Eng.* 2000; **R28**: 1–63; (b) Ray SS, Okamoto M. Polymer/layered silicate nanocomposites: A

review from preparation to processing. *Prog. Polym. Sci.* 2003; **28**: 1539–1641; (c) Giannelis EP, Krishnamoorti RK, Manias E. Polymer-silicate nanocomposites: Model systems for confined polymers and polymer brushes. *Adv. Polym. Sci.* 1998; **138**: 107–148.
2. Kojima Y, Usuki A, Kawasumi M, Okada A, Fukushima Y, Karauchi T, Kamigaito O. Synthesis of nylon 6-clay hybrid by montmorillonite intercalated with ε-caprolactam. *J. Polym. Sci. Part A: Polym. Chem.* 1993; **31**: 983–986.
3. Zhu J, Morgan AB, Lamelas FJ, Wilkie CA. Fire properties of polystyrene-clay nanocomposites. *Chem. Mater.* 2001; **13**: 3774–3780.
4. Gilman JW, Jackson CL, Morgan AB, Harris R, Manias E, Giannelis EP, Wuthenow M, Hilton D, Phillips SH. Flammability properties of polymer-layered-silicate nanocomposites. Polypropylene and polystyrene nanocomposites. *Chem. Mater.* 2000; **12**: 1866–1873.
5. Zhu J, Uhl FM, Morgan AB, Wilkie CA. Studies on the mechanism by which the formation of nanocomposites enhances thermal stability. *Chem. Mater.* 2001; **13**: 4649–4654.
6. Du J, Zhu J, Wilkie CA, Wang J. An XPS investigation of thermal degradation and charring on PMMA clay nanocomposites. *Polym. Degrad. Stab.* 2002; **77**: 377–381.
7. Du J, Wang J, Su S, Wilkie CA. Additional XPS studies on the degradation of poly(methyl methacrylate) and polystyrene nanocomposites. *Polym. Degrad. Stab.* 2004; **83**: 29–34.
8. Du J, Wang D, Wilkie CA, Wang J. An XPS study of the thermal degradation and flame retardant mechanism of polystyrene-clay nanocomposites. *Polym. Degrad. Stab.* 2002; **77**: 249–252.
9. Jang BN, Wilkie CA. The effect of clay on the thermal degradation of polyamide 6 in polyamide 6/clay nanocomposites. *Polymer* 2005; **46**: 3264–3274.
10. Jang BN, Wilkie CA. The thermal degradation of polystyrene nanocomposites. *Polymer* 2005; **46**: 2933–2942.
11. Costache M, Wilkie CA. Thermal degradation of ethylene-vinyl acetate copolymer nanocomposites. *Polymer* 2005; **46**: 6947–6958.
12. Jang B, Wilkie CA. The effects of clay on the thermal degradation behavior of poly(styrene-co-acrylonitirile), *Polymer* 2005; **46**: 9702–9713.
13. Jang B, Costache M, Wilkie CA. The relationship between thermal degradation behavior of polymer and the fire retardancy of polymer/clay nanocomposites. *Polymer* 2005; **46**: 10678–10687.
14. Leroux F, Besse JP. Polymer interleaved layered double hydroxide: A new emerging class of nanocomposites. *Chem. Mater.* 2001; **13**: 3507–3515.
15. Prinetto F, Ghiotti G. Investigation on acid-base properties of catalysts obtained from layered double hydroxides. *J. Phys. Chem. B* 2000; **104**: 11117–11126.
16. Costantino U, Marmottini F, Nocchetti M, Vivani R. New synthetic routes to hydrotalcite-like compounds-characterisation and properties of the obtained materials. *Eur. J. Inorg. Chem.* 1998; **10**: 1439–1446.
17. Ogawa M, Kaiho H. Homogeneous precipitation of uniform hydrotalcite particles. *Langmuir* 2002; **18**: 4240–4242.
18. Bender Koch C. Structure and properties of anionic clay minerals. *Hyperfine Interact.* 1998; **117**: 131–157.
19. Kashiwagi T, Inaba A, Brown EJ. Effects of weak linkages on the thermal and oxidative degradation of poly(methyl methacrylates). *Macromolecules* 1986; **19**: 2160–2168.
20. Inaba A, Kashiwagi T, Brown EJ. Effects of initial molecular weight on thermal degradation of poly(methyl methacrylate). Part 1. Model 1. *Polym. Degrad. Stab.* 1988; **21**: 1–20.
21. Kashiwagi T, Inaba A. Behavior of primary radicals during thermal degradation of poly(methyl methacrylate). *Polym. Degrad. Stab.* 1989; **26**: 161–184.
22. Manring L. Thermal degradation of poly(methyl methacrylate). 4. Random side-group scission. *Macromolecules* 1991; **24**: 3304–3309.
23. McNeill IC. A study of the thermal degradation of methyl methacrylate polymers and copolymers by thermal volatilization analysis. *Eur. Polym. J.* 1968; **4**: 21–30.
24. Zhu J, Start P, Mauritz KA, Wilkie CA. Thermal stability and flame retardancy of poly(methyl metrhacrylate)-clay nanocomposites. *Polym. Degrad. Stab.* 2002; **77**: 253–258.
25. Jash P, Wilkie CA. Effects of surfactants on the thermal and fire properties of poly(methyl methacrylate)/class nanocomposites. *Polym. Degrad. Stab.* 2005; **88**: 401–406.
26. Wang D, Zhu J, Yao Q, Wilkie CA. A comparison of various methods for the preparation of polystyrene and poly (methyl methacrylate) clay nanocomposites. *Chem. Mater.* 2002; **14**: 3837–3843.
27. Chen W, Feng L, Qu B. In situ synthesis of poly(methyl methacrylate)/MgAl layered double hydroxide nanocomposite with high transparency and enhanced thermal properties. *Solid State Commun.* 2004; **130**: 259–263.
28. Park SJ, Cho MS, Lim ST, Choi HJ, Jhon MS. Synthesis and dispersion characteristics of multi-walled carbon nanotube composites with poly(methyl methacrylate) prepared by *in situ* bulk polymerization. *Macromol. Rapid Commun.* 2003; **24**: 1070–1073.
29. Gilman JW, Kashiwagi T, Nyden M, Brown JET, Jackson CL, Lomakin S, Gianellis EP, Manias E. Flammability studies of polymer layered silicate nanocomposites: Polyolefin, epoxy and vinyl ester resins. In *Chemistry and Technology of Polymer Additives*, Al-Maliaka S, Golovoy A, Wilkie CA (eds). Blackwell Scientific: London, 1998; 249–265.
30. Su S, Jiang DD, Wilkie CA. Polybutadiene-modified clay and its polystyrene nanocomposites. *J. Vinyl Add. Technol.* 2004; **10**: 44–51.
31. Su S, Jiang DD, Wilkie CA. Poly(methyl methacrylate), polypropylene and polyethylene nanocomposites formation by melt blending using novel polymerically-modified clays. *Polym. Degrad. Stab.* 2004; **83**: 321–331.
32. Su S, Wilkie CA. Exfoliated poly(methyl methacrylate) and polystyrene nanocomposites occur when the clay cation contains a vinyl monomer. *J. Polym. Sci. Part A: Polym. Chem.* 2003; **41**: 1124–1135.
33. Camino G, Maffezzoli A, Braglia M, De Lazzaro M, Zammarano M. Effect of hydroxides and hydroxycarbonate structure on fire retardant effectiveness and mechanical properties in ethylene-vinyl acetate copolymer. *Polym. Degrad. Stab.* 2001; **74**: 457–464.
34. Kashiwagi T, Du F, Winey KI, Groth KM, Shields JR, Bellayer SP, Kim H, Douglas JF. Flammability properties of polymer nanocomposites with single-walled carbon nanotubes: Effects of nanotube dispersion and concentration. *Polymer* 2005; **46**: 471–481.